SEVENTH EUROPEAN ROTORCRAFT AND POWERED LIFT AIRCRAFT FORUM

Paper No. 10

DYNAMIC AND AEROELASTIC CHARACTERISTICS OF COMPLETE WINDTURBINE SYSTEMS

E. Steinhardt

Hochschule der Bundeswehr
München, F.R.G.

September 8 - 11, 1981

Garmisch-Partenkirchen
Federal Republic of Germany

Deutsche Gesellschaft für Luft- und Raumfahrt e. V.
Goethestr. 10, D-5000 Köln 51, F.R.G.

DYNAMIC AND AEROELASTIC CHARACTERISTICS OF COMPLETE WINDTURBINE SYSTEMS

E.W. Steinhardt

Institut für Luftfahrttechnik und Leichtbau
Hochschule der Bundeswehr München, F.R.G.

ABSTRACT

For the investigation of the dynamic and aeroelastic characteristics of large horizontal axis windturbines a hybrid model consisting of rigid bodies and flexible continuous structures was developed. Degrees of freedom include tower bending and torsion, pitch and yaw of the nacelle as well as rotation, inplane and out-of-plane bending of the blades. Aerodynamic forces are introduced with special regard on motion-induced effects and on gusts.
A set of partial integro-differential equations was established via the principle of virtual work. The application of Galerkin's extended method gives a system of linear periodic differential equations.
The numerical results confirm strong rotor-tower-coupling and illustrate the typical features of periodic systems. Instationary aerodynamic terms are found to be of minor importance and hingeless rotors will be damped better than teetering rotors, but tower and blade reactions to gravity and gusts are higher.

1. Introduction

As well as the primary energy resource 'wind' is unlimited and free, wind energy converters have to compete with conservative power plants. This economical demand naturally effects the dimensions and the configuration of windturbines. Units of 3 MW have rotors of 100 metres diameter which are fixed at towers of 100 metres height. Furthermore, only horizontal axis windturbines with one or two blades seem to be practicable for large systems[1,2] (see Fig. 1). Economical effectivity can be reached only if these units do work with extreme reliability over a lot of years. This means that there is no danger of dynamic or aeroelastic instability and response loading on external forces can be kept small.

Problems concerning the substructures, like isolated blades[3,4,5,6], complete rotors[7] , wire-stiffened towers etc., can be regarded as solved, because there exist a lot of very high qualified theories and computer codes for helicopter blades. Effects from coupling of an elastic rotor-system, fixed on an elastic tower will influence the behaviour of such windturbines essentially. This is a problem very similar to that of tilt-wing aircraft leading to rotor-whirl-flutter. A considerable amount of research has been done on that subject[8-10]. So, computer codes for helicopters and tilt-wing aircrafts were modified and applied to

windturbines[11,12].
In addition several programs for combined rotor-tower-motion of windturbines were developed in the last few years[13-17]. They are based on helicopter-fuselage-rotor models[16] or FE-methods[14] and branch-mode methods[15] and use quasistatic aerodynamics. Ref. 16 includes even nonlinear effects.
The intention of the presented study[18] is to find a simple mechanical and aerodynamic model which represents, in a realistic manner, especially the dynamic and aeroelastic characteristics of complete windturbines using a minimum of parameters.

2. Modeling

Modeling a complete windturbine depends on the object to be analysed. Exact data of the wings' airfoils and geometry as well as inflow theories are necessary for the computation of power, thrust and rotational speed. Under certain circumstances the flutter of isolated blades can only be predicted if nonlinear theories are used. In contrary, for dynamic and aeroelastic stability and response of the complete system these data can be simplified while additional structural data, instationary aerodynamics, gravity and gusts have to be taken into account.
So a hybrid model was used to represent a complete windturbine. Hybrid means, it can be divided into rigid bodies, like nacelle and rotor head, and elastic continuous structures, like tower and rotor blades. To keep the number of parameters small, further assumptions and simplifications were introduced. These are the most important:

- Deformations are small compared with blade length.
- Tower and blades are idealized as cantilevered beams of constant mass and stiffness.
- The stiffness of the guying wires is included in tower stiffness.
- The nacelle is rigidly attached to the tower.
- The rolling of the nacelle can be neglected and the rotor has constant rotational speed.
- The blade element theory is valid and aerodynamic forces act on rotor blades only.
- The center of gravity, the elastic axis and the aerodynamic center of the blade are congruent.
- Small blade twist is assumed within aerodynamic region.
- Aerodynamical drag doesn't influence dynamic behaviour.

3. Kinematics

Degrees of freedom of the hybrid model include translations and rotations of the rigid bodies and deformations of the continua which are dependent on time and position (see Fig. 2). Rigid body motions are two perpendicular nacelle translations in the horizontal plane, pitch and yaw as well as the rotation Ψ and rigid flapping of the rotor head $\beta_s(t)$. The tower bending and torsion are connected with nacelle motions by compatibility conditions. Blades are fixed with a δ_3-angle and are preconed. Inplane and out-of-plane bending is included, too. Since the blade torsion's influence on windturbines' total behaviour is small, it was neglected. In the case of one-bladed turbines a balance mass is fixed at the rotor head.
The position of every point of the turbine can be formulated in an inertial system by a series of translations and rotations as follows:

$$ {}_I\underline{r}_P = {}_I\underline{r}_G + {}_I\underline{v}_G + \overset{11}{\underline{\underline{S}}}\cdot\left[{}_1\underline{r}_R + \overset{16}{\underline{\underline{S}}}\cdot\left({}_\delta\underline{r}_B + {}_\delta\underline{v}_B + \overset{45}{\underline{\underline{S}}}\cdot {}_5\underline{r}_P \right) \right] , \qquad (1) $$

where ${}_I\underline{r}_G$, ${}_1\underline{r}_R$ and ${}_\delta\underline{r}_B$ denote the position of undeformed nacelle, rotor and

blade element, $_{I}\underline{v}_{G}$ and $_{\delta}\underline{v}_{B}$ are standing for translative deformations and $^{11}\underline{S}$, $^{16}\underline{S}$ and $^{45}\underline{S}$ for rotations. Defining a hybrid coordinate vector

$$\underline{p}_h(r,{}_T y,t) = \left[\, \underline{p}_G^T(t),\ \beta_s(t),\ \underline{p}_B^T(r,t),\ \underline{p}_T^T({}_T y,t) \,\right]^T, \tag{2}$$

which includes rigid body motions $\underline{p}_G(t)$ of the nacelle, $\beta_s(t)$ the rigid flapping, the displacements of blade I $\underline{p}_B(r,t)$ and tower $\underline{p}_T({}_T y,t)$, the vectors of translative velocities

$$_{I}\underline{u}_P(r,{}_T y,t) = \underline{\underline{J}}_{trans}(\underline{p}_h,t)\cdot\underline{p}_h(r,{}_T y,t) + \frac{\partial}{\partial t}({}_{I}\underline{r}_P) \tag{3}$$

and the angular velocities

$$_{I}\underline{\omega}_P(r,{}_T y,t) = \underline{\underline{J}}_{rot}(\underline{p}_h,t)\cdot\underline{p}_h(r,{}_T y,t) + \frac{\partial}{\partial t}(\underline{s}_P) \tag{4}$$

in the inertial system are following from (1). The compatibility condition

$$\underline{p}_G(t) = Q_K(\underline{p}_T(H,t)) \tag{5}$$

expresses nacelle motions by the deformation of the top of the tower.

4. Aerodynamics

Aerodynamic forces acting on a rotor blade at radial station r can be classified into internal forces and external forces.

Internal forces are produced by the flapping h(r,t) and pitching α(r,t) of a blade section relative to the stationary inflow (see Fig. 3). The downwash at each point of the airfoil can be expressed by equations (3) and (4). and formulated as

$$\begin{aligned} h(r,t) &= \underline{h}^T(r,t)\cdot\underline{p}_h(r,t) \quad , \\ \alpha(r,t) &= \underline{\alpha}^T(r,t)\cdot\underline{p}_h(r,t) \quad . \end{aligned} \tag{6}$$

Stationary inflow angle $\tilde{\lambda}(r)$ following from the simple momentum theory gives the effective velocity

$$V_\infty(r,t) = r\Omega\cdot(\ 1 + 0.5\tilde{\lambda}^2(r)\ ). \tag{7}$$

While quasistatic aerodynamics usuallly use the motion induced downwash only to get an effective inflow angle and a resultant velocity, in this paper virtual mass effects and circulatory effects are included, too. As the motion is not necessarily periodic, transient movements must be allowed. Therefore the definition of lag functions $B_k(r,t)$ is very convenient.[19,20] The lift force per unit acting on a blade element is then given by

$$\begin{aligned} f_a(r,t) = &- \mathfrak{C}_a\cdot\frac{\rho}{2}\cdot c(r)\cdot\left[\ddot{h}(r,t) - a\cdot\ddot{\alpha}(r,t) - V_\infty(r)\cdot\dot{\alpha}(r,t)\right] + \\ &- \mathfrak{C}_a\cdot\rho\cdot c(r)\cdot V_\infty(r)\left[\, w_{3/4}(r,t) - \sum_1^2 B_k(r,t)\right] \quad , \end{aligned} \tag{8}$$

and the lag functions hold the partial differential equation

$$\dot{B}_k(r,t) + \beta_k\frac{V_\infty}{c(r)}\cdot B_k(r,t) = \dot{w}_{3/4}(r,t), \quad k = 1,2 \quad . \tag{9}$$

It must be emphasized that lag functions themselves are functions of radius and time according to the downwash $w_{3,4}(r,t)$.

External aerodynamic forces do not depend on the deformations of the windmill. They are caused by atmospheric conditions. Natural wind $V_W(y,t)$ can be separated into a constant flow V_0, into a part which as a result of boundary layer is only variing with height and into gusts where velocity changes with position and time (see Fig. 4). From the view of the rotating blade element the boundary layer effect can be treated like gusts. The lift force of a gust field on a blade element is

$$f_{Gust}(r,t_{Gust}) = - c_a \cdot \frac{\rho}{2} \cdot V_\infty^2(r) \cdot 2 \cdot c(r) \cdot I_{Gust}(r,t_{Gust}) \ , \tag{10}$$

where $I_{Gust}(r,t)$ denotes the gust integral

$$I_{Gust}(r,t) = \int_0^{t_{Gust}} \frac{\partial}{\partial \tau} \left(\frac{V_{Gust}(r,\tau)}{V_\infty(r)} \right) \cdot \tilde{K}(r, t_{Gust} - \tau) \ d\tau \tag{11}$$

and Kuessner's function is approximately

$$\tilde{K}(r,t) = 1 - \sum_3^4 a_k \cdot \exp\left(-\beta_k \cdot \frac{V_\infty(r)}{c(r)} t \right) . \tag{12}$$

Similar to the lag functions the gust integrals depend on radial location, too.

5. Equations of motion

The equations of motion are derived via the extended Hamiltons's principle or principle of virtual work as nonconservative forces are acting on the system:

$$\int_{t_1}^{t_2} (\delta T - \delta U + \delta W_{nc}) \cdot dt = 0 \ . \tag{13}$$

The main advantages of this energy principle are that it is independent of the coordinate system and that boundary conditions follow automatically. Equations (3) and (4) together with inertia parameters provide the total kinetic energy T of the blade, the tower, the rotor head, the nacelle and, as far as necessary, of the balancing mass. The potential energy U includes the elastic potential of the blade, the tower and the teetering hinge as well as the centrifugal and gravity potential. The virtual work of the nonconservative forces δW_{nc} contains material damping, viscous damping of the hinge and aerodynamic forces, which are working on the displacements $h(r,t)$ and $\alpha(r,t)$ of the blade elements.
Performing the variation (13) provides a so-called integro-differential equation system:

$$\begin{aligned} & D_S(\underline{p}_S) \cdot \delta \underline{p}_S + \int_{R_0}^{R} D_a(\underline{p}_h, \underline{p}_L) \cdot \delta \underline{p}_h \ dr + \\ & + \int_{R_0}^{R} \{ D_B(\underline{p}_B) \cdot \delta \underline{p}_B + D_{BS}(\underline{p}_B, \underline{p}_S) \cdot \delta \underline{p} \} \cdot dr + \{ C_B(\underline{p}_B) \cdot \delta \underline{p}_B' + \overset{'}{C}_B(\underline{p}_B) \cdot \delta \underline{p}_B \} \Big|_{R_0}^{R} + \\ & + \int_0^H \{ D_T(\underline{p}_T) \cdot \delta \underline{p}_T \} d_T y + \{ C_T(\underline{p}_T) \cdot \delta \overset{\Delta}{\underline{p}}_T + \overset{\Delta}{C}_T(\underline{p}_T) \cdot \delta \underline{p}_T \} \Big|_0^H = 0 \ . \end{aligned} \tag{14}$$

It is distinguished analogous to the hybrid model by differential operators $D_S(\underline{p}_S,t)$, according to the rigid bodies, and partial differential operators $D_B(\underline{p}_B,r,t)$, $D_T(\underline{p}_T)$, according to the elastic continua, which are to be fulfilled over the whole domain. The virtual work of the aerodynamic forces can be written as an integral over a partial differential operator, too. Additionally the virtual work at the boundaries, denoted by $C_B(\underline{p}_B)\cdot\delta\underline{p}_B$ etc. is to be taken into account.
Inserting equations (6) into (9) gives a partial differential equation system $D_L(p_L,p_h,t)$. In order to eliminate spatial dependence it is integrated over the total blade length and one can write:

$$\int_{R_o}^{R} D_L(\underline{p}_L,\underline{p}_h,r,t)\,dr = 0. \tag{15}$$

Now, equations (5), (14) and (15) describe the dynamic and aeroelastic behaviour of a complete one-bladed windturbine.

An approximate numerical solution can be obtained by application of the extended Galerkin's method, which converges even in the case of nonconservative, nonselfadjoint problems and for admissable functions. Blade and tower deflections can be transformed then into generalized coordinates $\underline{q}_B(t)$, $\underline{q}_T(t)$ by

$$\begin{aligned}\underline{p}_B(r,t) &= \underline{\underline{\Phi}}_B(r)\cdot\underline{q}_B(t)\ ,\\ \underline{p}_T({}_Ty,t) &= \underline{\underline{\Phi}}_T({}_Ty)\cdot\underline{q}_T(t)\ ,\end{aligned} \tag{16}$$

where the matrices $\underline{\underline{\Phi}}_B(r)$ and $\underline{\underline{\Phi}}_T({}_Ty)$ contain admissible functions. The lag functions are also generalized introducing

$$\underline{p}_L(r,t) = \underline{\underline{\Phi}}_L(r)\cdot\underline{q}_L(t)\ , \tag{17}$$

but it is not evident how to find modal lag functions.

Selecting a special reduced set of modal tower functions it is possible to eliminate generalized tower coordinates. Then there exists the inverse of equation (5)

$$\underline{p}_T({}_Ty,t) = \underline{\underline{\Phi}}_K(H,{}_Ty)\cdot\underline{q}_G(t), \tag{18}$$

which expresses tower deformation in nacelle coordinates.

After introduction of equations (16) to (18) into (14) and (15), replacing the time by a nondimensional angle of elevation $\Psi = \delta_3 + \Omega\,t$ and dividing them through $MR^2\Omega^2$ we get two sets of second-order ordinary differential equations:

$$\underline{\underline{M}}_\eta(\Psi)\cdot\ddot{q}(\Psi) + \underline{\underline{D}}_\eta(\Psi)\cdot\dot{q}(\Psi) + \underline{\underline{K}}_\eta(\Psi)\cdot q(\Psi) - \underline{L}(\Psi)\cdot q_L(\Psi) - \underline{F}_\eta(\Psi) = 0\ , \tag{19}$$

$$-\underline{\underline{M}}_L(\Psi)\cdot\ddot{q}(\Psi) - \underline{\underline{D}}_L(\Psi)\cdot\dot{q}(\Psi) - \underline{\underline{K}}_L(\Psi)\cdot q(\Psi) + \underline{L}_1\dot{q}_L(\Psi) + \underline{L}_2 q_L(\Psi) = 0\ . \tag{20}$$

All matrices except $\underline{L}_1$ and $\underline{L}_2$ are periodic. $\underline{\underline{M}}_\eta(\Psi)$, $\underline{\underline{D}}_\eta(\Psi)$ and $\underline{\underline{K}}_\eta(\Psi)$ contain aerodynamic and structural terms. The latter include gyroscopic and gravity effects. The vector $\underline{F}_\eta(\Psi)$ combines all external forces, like gravity, centrifugal, constant wind and gust force. The matrices $\underline{L}$, $\underline{\underline{M}}_L$, $\underline{\underline{D}}_L$, $\underline{\underline{K}}_L$, $\underline{L}_1$ and $\underline{L}_2$ represent instationary aerodynamics.

As the matrix

$$\underline{\underline{P}} = \begin{bmatrix} \hat{\underline{\underline{P}}}_S + & \vdots & \hat{\underline{\underline{P}}}_{SB} \\ + \hat{\underline{\underline{\Phi}}}_K^T \hat{\underline{\underline{P}}}_T \hat{\underline{\underline{\Phi}}}_K & \vdots & \\ \cdots\cdots & \vdots & \cdots\cdots \\ \hat{\underline{\underline{P}}}_{BS} & \vdots & \hat{\underline{\underline{P}}}_B \end{bmatrix} \qquad (21)$$

standing for $\underline{\underline{M}}_n$, $\underline{\underline{D}}_n$ or $\underline{\underline{K}}_n$ shows, it can be subdivided into $\hat{\underline{\underline{P}}}_S$ describing the rigid bodies, $\hat{\underline{\underline{P}}}_B$ representing the blades and $\hat{\underline{\underline{P}}}_{BS}$, $\hat{\underline{\underline{P}}}_{SB}$ are responsible for rotor - tower coupling. The coupling is caused essentially by changes of inertia parameters (unbalance) as a result of elastic deformations, by gravitational stiffness and by aerodynamics. If (18) is valid the modal tower parameters are added to nacelle area of $\underline{\underline{P}}$.
Equations (19) and (20) can be transformed into a first-order differential equation system

$$\underline{x}(\Psi) = \underline{\underline{A}}(\Psi) \cdot \underline{x}(\Psi) + \underline{e}(\Psi) \quad , \qquad (22a)$$

where $\underline{x}(\Psi)$ denotes the state vector

$$\underline{x} = \{\underline{q}^T , \underline{\dot{q}}^T , \underline{q}_L^T\}^T . \qquad (22b)$$

6. The Two-Bladed Teetering Rotor

The equations of motion of two-bladed windturbines can be derived from those of one-bladed rotors, taking into account geometric constraints. Furthermore it is comfortable and illustrative to define new symmetrical and antimetrical blade deformations as the sum or the difference of single blade coordinates (see Fig. 5a) and to separate local gusts like Fig. 5b shows:

$$\begin{aligned} w^s(r,t) &= 0.5\cdot(w^I(r,t) + w^{II}(r,t)), \\ w^a(r,t) &= 0.5\cdot(w^I(r,t) - w^{II}(r,t)), \\ u^s(r,t) &= 0.5\cdot(u^I(r,t) - u^{II}(r,t)), \\ u^a(r,t) &= o.5\cdot(u^I(r,t) + u^{II}(r,t)). \end{aligned} \qquad (23)$$

This definition has to be extended to lag functions. Geometric and kinematic conditions define the generalized coordinates of the two-bladed turbine as

$$\underline{z} = \underline{\underline{T}} \cdot \begin{bmatrix} \underline{q}^I \\ \underline{q}^{II} \end{bmatrix} \quad , \qquad \underline{z}_L = \underline{\underline{T}}_L \cdot \begin{bmatrix} \underline{q}_L^I \\ \underline{q}_L^{II} \end{bmatrix} \qquad (24)$$

and the matrices as

$$\underline{\underline{P}}^{(2)} = \underline{\underline{T}}^T \cdot \begin{bmatrix} \underline{\underline{P}}_S + \underline{\underline{P}}^I & \vdots \\ \cdots\cdots & \vdots \\ \vdots & \underline{\underline{P}}^{II} \end{bmatrix} \cdot \underline{\underline{T}} \quad , \qquad (25)$$

where $\underline{P}_S$ denotes all parameters of rigid bodies and tower and $\underline{P}^{II}$ is the modified blade matrix $\underline{P}^{I}$ according to the geometric conditions. The equations of motion are of the same structure as equations (19) and (20).

7. Results

The linear first-order differential equation system can be analysed by numerical integration. A special digital computer program (see Fig. 6), which is suited for stability analysis as well as for response problems was developed and applied to an example, whose parameters are quite similar to those of GROWIAN I.

The exact solutions of a cantilevered beam have been selected as assumed functions, the first two modes representing elastic flapping and the first one inplane bending. So we have 11 generalized structural coordinates and 4 generalized lag coordinates.

Several integration modes for the computation of the monodromy matrix have been tested. With the method suggested by Friedmann[23] good results could be reached within 275 s, while variable step size methods of higher order needed 420 s to 1300 s for results of the same accuracy. But it must be emphasized that this is only true if an optimum stepsize, which depends on system parameters, can be found.

7.1 Snapshot method

A periodic system is stable if the condition $|\mu| < 1$ holds true for all eigenvalues of the monodromy matrix $\Gamma(2\pi, 0)$. The computation of this matrix for different parameters takes a considerable amount of computer time. So it can be helpful to apply the so-called snapshot method[14], where the state of the system (inclusive gyroscopic forces) is frozen in a destinct rotor position Ψ_0. The eigenvalues and eigenvectors of the problem with now constant parameters can be found easily. Although this method contradicts physical reality, it gives a good idea of frequencies and modes of the system. Fig. 7a shows the natural frequencies against rotational speed of the complete rotor-tower system, and in Fig. 7b those of the same rotor on a rigid tower are plotted, both without aerodynamics. What can we learn from this method?

- The 'frequencies' and 'modes' vary with rotational speed and rotor position and differ from those of the substructures.
- Teetering rotors on elastic towers have 'frequencies' $\omega_i / \Omega < 1$.
- Strong rotor-tower coupling influences 'frequncies' and 'modes'.
- Crossing points of rotor harmonics and equivalence of frequencies may be sensitive to parameter and combination resonance. These points are to be examined exactly, because
- stability cannot be determined from the eigenvalues of the snapshot method.

7.2 Stability

The monodromy matrix $\Gamma(2\pi, 0)$ is equivalent to the response of the system after one revolution on a unity deflection of the corresponding coordinate. Fig. 8 shows the state of the system during a complete rotation, which refers to the first column of $\Gamma(\Psi, 0)$. It can be seen that an initial radial

tower deflection shifts energy to the symmetrical inplane motion. However, the increasing amplitude of this mode is actually no instability, as it is decreasing later on again. Stability can be proofed only following Floquet's theory. Furthermore, symmetrical inplane bending stimulates also rigid flapping and yawing, caused by inertia and gyroscopic coupling. This underlines the fact of strong rotor-tower coupling, too. These 'almost periodic' motions are characteristic features of periodic systems. In addition, this makes clear that the transformed eigenvalues according to Liapunov's theorem of reducibility

$$\lambda = \rho + i\omega = \frac{\Omega}{2\pi} \left(\ln|\mu| + i \arctan \frac{\mathrm{Im}(\mu)}{\mathrm{Re}(\mu)} \right) \qquad (26)$$

cannot give a complete imagination of the turbines' motion.

Instabilities can be produced by dynamic or aeroelastic effects.

Dynamic instabilities are well-known effects in rotating machinery. They are caused by unsymmetric rotors which lead to parametric systems and can be observed for windmills with one or two blades, too. [24],[25] For hinged or elastic deformable rotor blades additional instabilities can be found, e.g. the well-known ground resonance. This effect is responsible for the isolated instabilities ($|\mu| > 1$) at $\Omega/\Omega_\varrho = 2.28$ in Fig. 9a and 9b. For the hypothetical case without aerodynamics another instability was found at $\Omega/\Omega_\varrho = 0.6$, but in Fig.9a it is completely damped. These instabilities appear only at isolated points and, because of the relatively wide parameter steps, the existence of further ones cannot be excluded.

Aerodynamics may effect stability behaviour in different ways. Virtual mass can alter the frequencies but its influence is found to be very small , whereas aerodynamic stiffness and damping can produce divergence and flutter. So, the teetering rotor turbine (Fig. 9a) shows rotor-whirl-flutter for Ω/Ω_ϱ greater than 2.1. From the eigenvectors follows that rigid flapping, yawing and pitching of the nacelle take part in this motion. The turbines' eigenvalues with fixed rotor head (Fig. 9b) are all less unity, so no whirl-flutter appears. The results are based on quasistatic aerodynamics. From some investigations using lag functions it can be supposed that they are destabilizing, but the results differ very much if other modal lag function are introduced.

7.3 Response

As an example for various external forces, the gust force produced by tower shadow shall be presented here. The gust is limited on a sector $\Delta\psi$, velocity contribution is constant along radial station and changes with the angle of elevation like $1 - \cos(2\pi\psi/\Delta\psi)$.

Modal gust forces are usually computed assuming a representative radius for Küssner's function [26], see (12). This method fails, however, for higher modes. That's why in the present paper time dependent modal gust forces were computed and tabulated. Figure 10 shows modal gust parameters.

The symmetrical modes, axial nacelle translation and symmetrical elastic bending respond with a nonharmonic periodic motion. The frequency is twice the frequency of rotation as can be recognized in Figure 11a.

The symmetrical modes' reactions are independent of the rotor head construction, whereas antimetrical modes differ essentially. For teetering rotors (Fig.11b) rigid flapping is excited mainly. This reduces elastic bending reactions about 100% compared with those of a fixed rotorhead turbine (Fig. 11c). The superposed motions of higher frequencies are caused by the second elastic flapping mode, which is also excited and coupled with rigid flapping. In

the case of rigid rotor head the yawing of the nacelle is greater.

So, from this point of view teetering rotor windturbines are preferable because of the compensating effect of the rigid flapping.

8. Conclusions

The developed hybrid model describes the characteristic behaviour of one or two bladed windturbines very well as the results confirm. It is suited for analysis of dynamic and aeroelastic stability as well as for response problems , like gravity, centrifugal forces, constant wind and deterministic gusts. The essential features of the method and some of the most interesting results shall be summarized below.

- The hybrid model is idealizing an elastic unsymmetrical rotor on an elastic tower.
- The analytical form of the linear equations support physical understanding and the estimation of the influence of parameters.
- The snapshot method can predict instabilities to a certain degree and so it is useful to save computer time for exact stability analysis.
- Instabilities caused by parametrical or combinatorical resonance may appear.
- Viscoelastic damping of tower and blades stabilizes the turbine to a certain amount.
- The introduction of lag functions and modal gust integrals takes into consideration instationary aerodynamic effects. In general quasistatic aerodynamics seems to be sufficient for motion induced effects.
- Aerodynamic forces can be stabilizing as well as destabilizing, depending on parameters. So teetering rotors are more sensitive for rotor-whirl-flutter than constructions with fixed rotor heads.
- On the other hand rotor blades and tower are loaded higher by gusts, if teetering motion cannot partially compensate such effects.

References

1. Helm, S., Erstellung baureifer Unterlagen für eine große Windenergieanlage GOWIAN I, Statusbericht Windenergie, VDI-Verlag, Düsseldorf, 1980
2. Meggle, R./ Schöbe, B., Programmübersicht GROWIAN II, Statusbericht Windenergie, VDI-Verlag, Düsseldorf, 1980.
3. Friedmann, P./ Tong, P., Non-Linear Flap-Lag Dynamics of Hingeless Helicopter Blades in Hover and Forward Flight, J.of Sound and Vibration, Vol. 30 (1973), No. 1, p. 9-31.
4. Friedmann, P., Influence of Structural Damping, Preconing, Offsets and Large Deflections on the Flap-Lag-Torsional Stability of a Cantilevered Rotor Blade. AIAA Paper 75-780, 1975.
5. Ham, N.D., Helicopter Blade Flutter, AGARD Report No. 607, in Manual of Aeroelasticity, Part III, Massachusetts Institute of Technologie, 1967.
6. Kottapalli, S./ Friedmann, P., Aeroelastic Stability and Response of Horizontal Axis Wind Turbine Blades, AIAA Journal, Vol. 17 (1979), No. 12, p. 1381-1389.

7. Shamie, J., Aeroelastic Stability of Complete Rotors with Application to a Teetering Rotor in Hover and Forward Flight, Ph.d. Thesis: Mechanic and Structures Dep. University of California, Los Angeles, 1976.

8. Loewy, G.R., Review of Rotary-Wing VSTOL Dynamic and Aeroelastic Problems, J. of AHS, Vol. 3 (1969), No. 3.

9. Kiessling, F., Übersicht zum Stand der Whirl-Flatter-Untersuchungen, DLR-FB 74-11, 1974.

10. Scheimann, J., Analytical Investigation of the Tilt Rotor Whirl Instability, Ph.D. Thesis, Virginia Polytechnic Institute and State University, 1972.

11. Hoffmann, J.A., Coupled Dynamics Analysis of Wind Energy Systems, NASA CR-135152, 1977.

12. Spera, D.A./ Jenetzke, D.C., Effects of Rotor Location, Coning and Gilt on Critical Loads of Large Turbines, NASA, Wind Technology Journal, Vol. 1 (1977), No. 1, p. 5-10.

13. Kiessling, F./ Rippl, M., Aeroelastische Versuche an Modellen von Windenergie-Konvertern, Vortrag anläßlich DGLR-Tagung des Fachausschusses 7.2, Bremen, 1980.

14. Otto, K.-P., Die Strukturdynamik des Voith-Windenergiekonverters, in Statusbericht Windenergie, VDI-Verlag, Düsseldorf, 1980.

15. Vollan, A., Garos - General Aeroelastic Analysis of Rotating Structures, User's Manual, Part 1, Theory, Hagnam, 1979.

16. Warmbrodt, W./ Friedmann, P., Formulation of the Aeroelastic Stability and Response Problem of Coupled Rotor/Support Systems, AIAA Paper 79-0732, Proceedings of the Twentieth AIAA/ASME/ASCE/AHS Structures, Structural Dynamics and Materials Conference, St. Louis, p. 39-52, April 1979.

17. Kehl, K./ Keim, W./ Kiessling, F./ Rippl, M., Zur Dynamik von großen Windkraftanlagen, in VDI-Berichte Nr. 381, VDI-Verlag, Düsseldorf, 1980.

18. Steinhardt, E., Zur Berechnung des dynamischen und aeroelastischen Stabilitäts- und Antwortverhaltens großer Windturbinen mit unsymmetrischem Rotor, Diss. ETH Zürich, to be published in late 1981.

19. Rodden, W.P./ Stahl, B., Strip Method for Prediction of Damping in Subsonic Wind Tunnel and Flight Flutter Tests, J. of Aircraft, Vol. 6 (1969), No. 1.

20. Strehlow, H./ Habsch, H., Weiterentwicklung aeroelastischer Rechenverfahren für Blattinstabilitätsuntersuchungen von Rotoren im Schnellflug, MBB-Bericht Nr. UD - 91 - 72, 1972.

21. Försching, H., Grundlagen der Aeroelastik, Berlin-Heidelberg-New York, 1974.

22. Leipholz, H., Über die Konvergenz des Galerkinschen Verfahrens bei nichtselbstadjungierten und nichtkonservativen Eigenwertproblemen, ZAMP, Nr. 14 (1963), S.70 ff.

23. Friedmann, P./ Hammond, C.E., Efficient Numerical Treatment of Periodic System with Application to Stability Problems, International J. for Numerical Methods in Engineering, Vol. 11 (1977), p. 1117-1136.

24. Müller, A., Einflüsse von Unsymmetrien auf das Bewegungsverhalten von Rotoren, Dissertation TU München, 1977.

25. Schweitzer, G., The problem of reducing the order of a large parametrically excited rotor system, presented at Rotorcraft Vibration Workshop, NASA Ames Research Center, 1978.

26. Ludwig, D., Allgemeine Lösungsmethode zur Ermittlung der dynamischen Antwort auf eine diskrete Einzelbö am Beispiel des Rotorblattes eines Windenergiekonverters, DFVLR-Forschungsbericht 80-12, Göttingen, 1980.

Appendix A: list of symbols

a	distance between elastic axis and chord center
a_k, β_k	coefficients of approximation for Wagner's function and Küssner's function
$\underline{\underline{A}}(\Psi)$	system matrix
$B_k(r,t)$	lag functions
$c(r)$	semi-chord length of blade element (B.E.)
c_a^{α}	lift curve slope
$C_i(\underline{p}_i)$	boundary condition operator
$D_i(\underline{p}_i)$	differential operator
$\underline{e}(\Psi)$	load vector
$f_a(r,t)$	lift force per unit length
$\underline{F}_n(\Psi)$	vector of normalized external forces
$h(r,t)$	effective flapping of B.E.
$\underline{h}(r,t)$	vector transforming common motion into effective flapping
H	height of tower
$I_{Gust}(r,t)$	gust integral
$\underline{\underline{J}}_{trans}$, $\underline{\underline{J}}_{rot}$	Jacobi's matrix of translation, rotation
$\tilde{K}(r,t)$	Küssner's function
$\underline{\underline{L}}$, $\underline{\underline{L}}_1$, $\underline{\underline{L}}_2$	lag matrices
$\underline{\underline{M}}_L$, $\underline{\underline{D}}_L$, $\underline{\underline{K}}_L$	" "
$\underline{\underline{M}}_n$, $\underline{\underline{D}}_n$, $\underline{\underline{K}}_n$	normalized matrices
$\underline{p}_B$, $\underline{p}_G$, $\underline{p}_S$, $\underline{p}_h$	vectors containing generalized coordinates
$\underline{\underline{P}}$, $\underline{\underline{\hat{P}}}_B$, $\underline{\underline{\hat{P}}}_{SB}$, $\underline{\underline{\hat{P}}}_{BS}$	formal matrices
$\underline{q}_B$, $\underline{q}_T$, $\underline{q}_G$, $\underline{q}$	vectors of generalized coordinates
$\underline{q}_L$	vector of generalized lag functions
Q_K	operator for tower nacelle coupling
r	radial station
R, R_o	outer, inner radius
${}_j\underline{r}_P$	position vector of point P in coordinate system j

$\underline{s}_p$	vector of rotation
$\underline{\underline{{}^{ij}S}}$	matrix of rotational transformation from system i to j
t	time
T	kinetic energy
$\underline{\underline{T}}$	transformation matrix for two bladed turbines
$u(r,t)$	inplane bending
$\underline{{}^{j}u}_p$	velocity vector
U	potential energy
$\underline{{}^{j}v}_p$	displacement vector
$V_\infty, V_0, V_w, V_{Gust}$	velocities of air flow
$w(r,t)$	out-of-plane bending
$w_{3/4}(r,t)$	downwash at 75% chord length
δW_{nc}	virtual work of nonconservative forces
$\underline{x}$	state vector
${}_T y$	tower coordinate
$\underline{z}, \underline{z}_L$	vectors of generalized coordinates of the two-bladed rotor
$\alpha(r,t)$	effective pitching of B.E.
$\underline{\alpha}(r,t)$	vector transforming common motion into effective pitching
$\beta_S(r,t)$	rigid flapping of rotor blade
δ_3	angle of teetering axes
$\lambda(r)$	inflow angle
λ_i	eigenvalue of $A(\Psi_0)$
μ_i	eigenvalues of the monodromy matrix
ρ	specific mass of air
ρ_i	real part of λ_i
τ	*dimensionless time*
$\underline{{}^{j}\omega}_p$	vector ao angular velocity
ω_i	natural frequencies
$\underline{\underline{\Gamma}}(\Psi,0)$	*monodromy matrix*
Ω, Ω_0	rotaional speed
$\underline{\underline{\Phi}}_i$	matrix of modal functions
Ψ	angle of elevation
$()^I, ()^{II}$	blade number
$()^s, ()^a$	symmetrical, antimetrical mode

$\dot{()} = \frac{\partial}{\partial t}(), \quad \hat{()} = \frac{\partial}{\partial {}_T y}(), \quad ()' = \frac{\partial}{\partial r}(), \quad ()^* = \frac{\partial}{\partial \Psi}()$.

Appendix B: List of figures

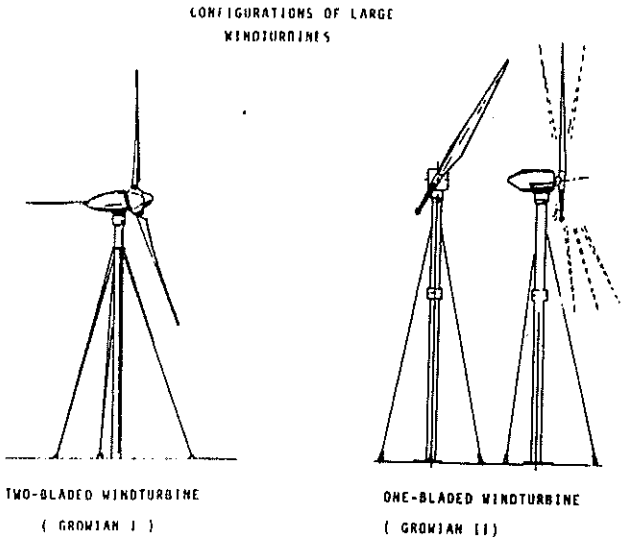

Fig. 1 Configurations of large wind energy converter projects.

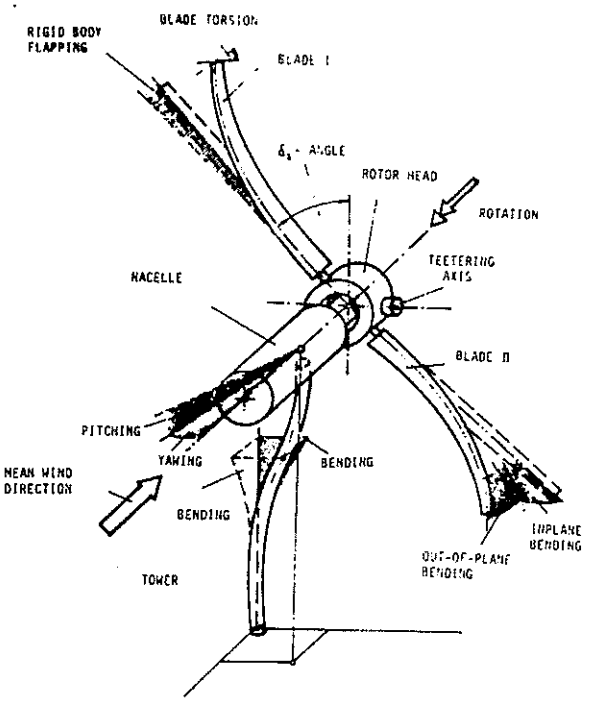

Fig. 2 Elements and degrees of freedom of the hybrid model

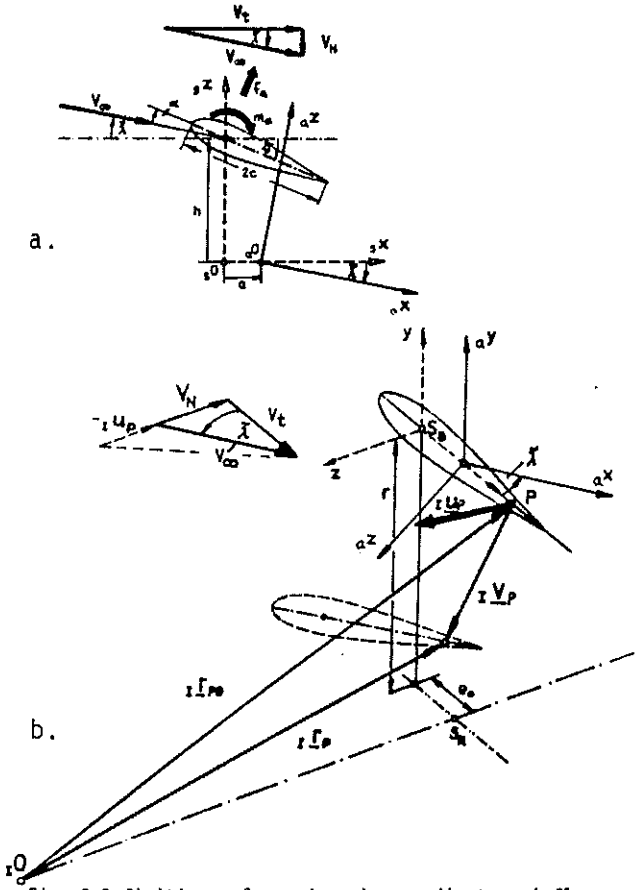

Fig. 3 Definitions of aerodynamic coordinates, inflow angle and effective flapping and pitching

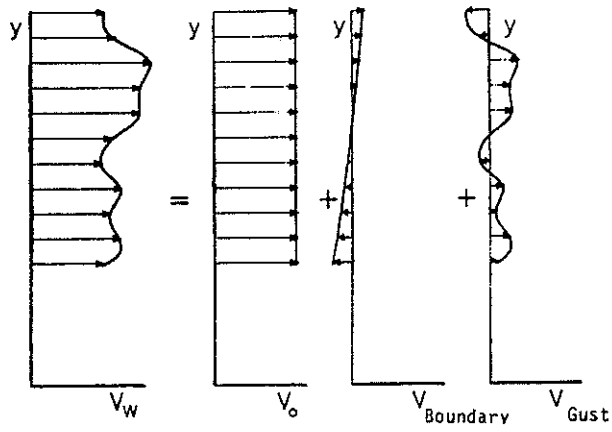

Fig. 4 Separation of natural wind into constant wind V_0, boundary layer effect $V_{Boundary}$ and gusts V_{Gust}.

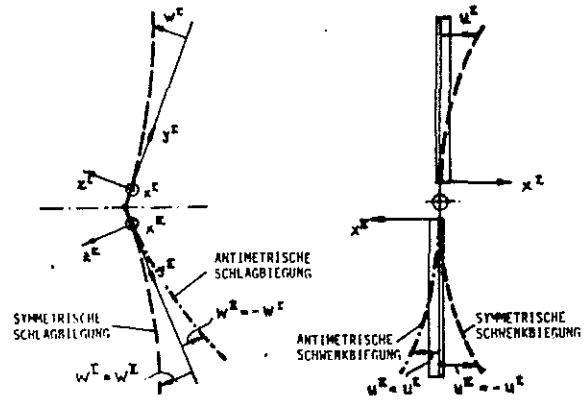

Fig. 5a Definition of symmetrical and antim etrical bending modes

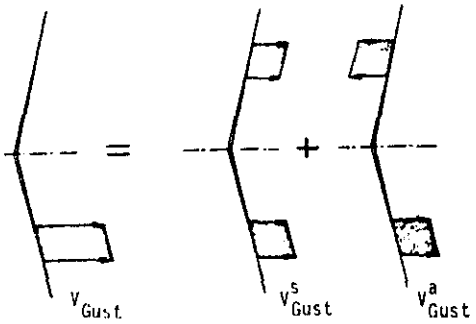

Fig. 5b Symmetrical and antimetrical gust separation for two-bladed turbines

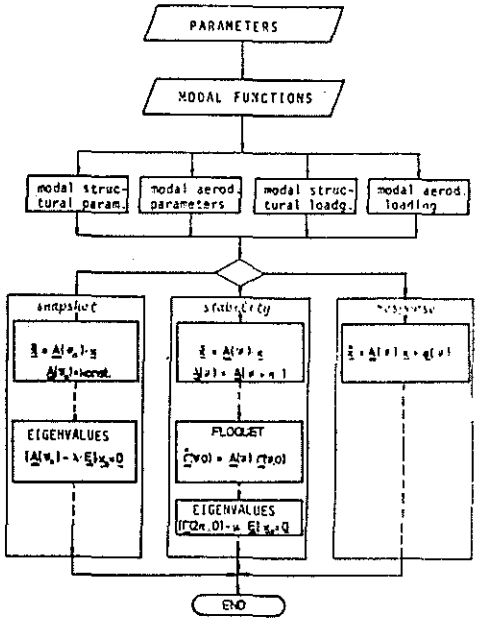

Fig. 6. Block diagram of the digital computer program

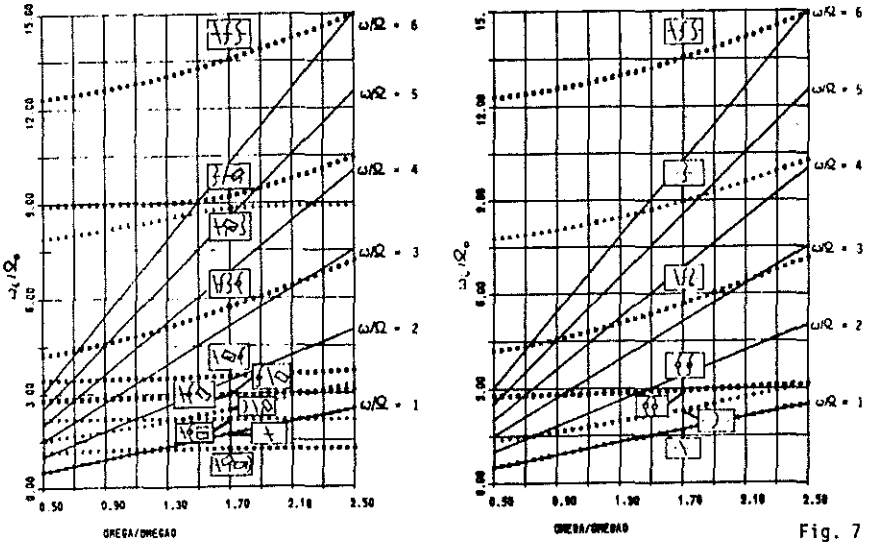

a. TEETERING ROTOR

b. RIGID TOWER

Fig. 7 Natural frequencies of the frozen system using snapshot method

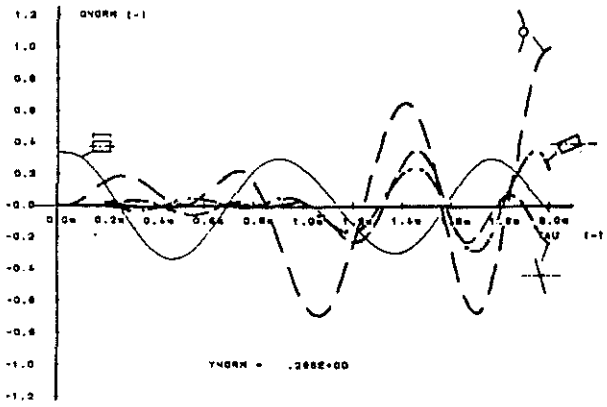

Fig. 8 System response on unity deflection of radial tower bending during the first period

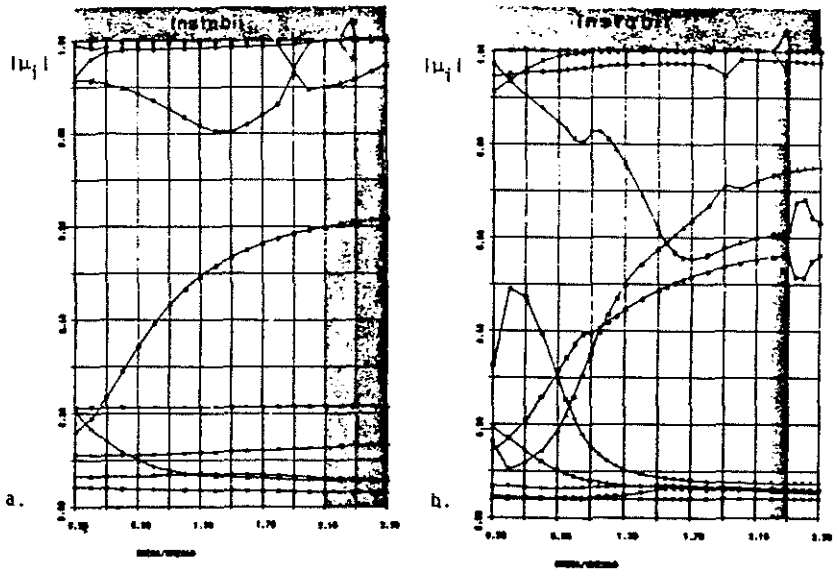

Fig. 9 Absolute length of the eigenvalues of the monodromy matrix and quasistatic aerodynamics

a. for teetering rotor head

b. for fixed rotor head.

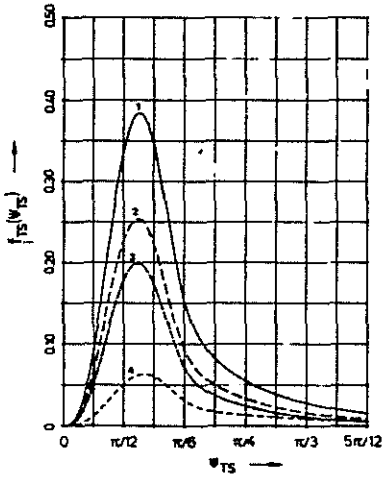

Fig. 10 Modal gust parameters of a 1 - cos gust over a 30^{0} sector.

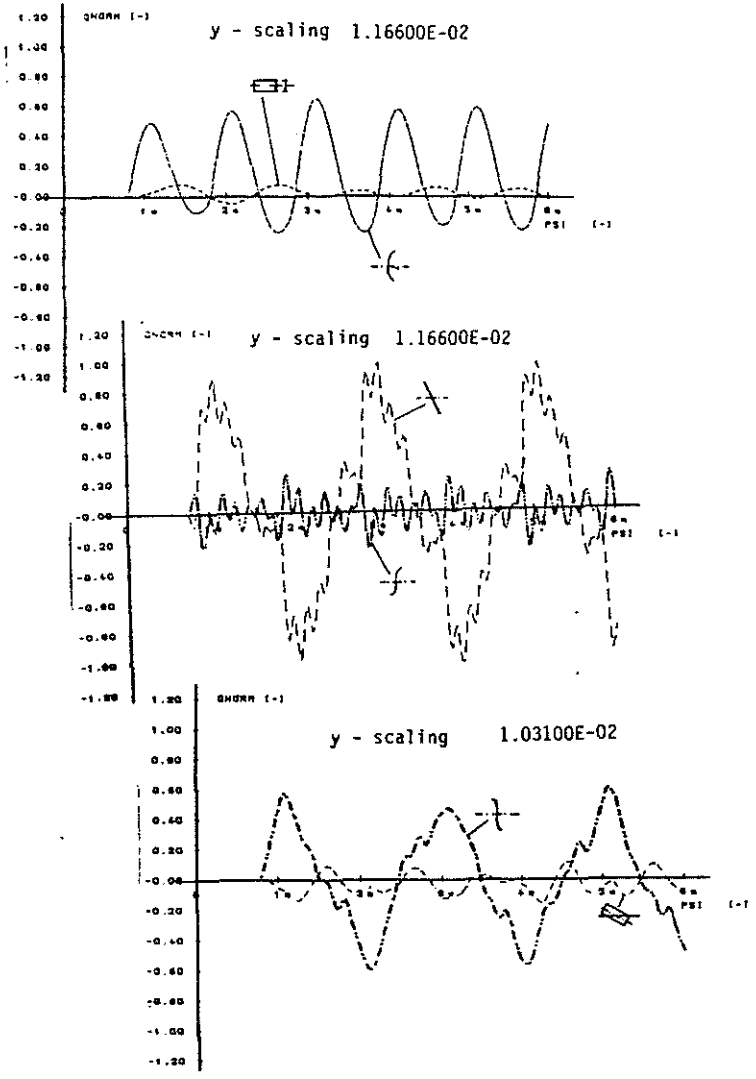

Fig. 11 Response on a 1-cos gust representing tower shodow on

a. symmetrical modes

b. antimetrical modes of teetering rotor turbine

c. antimetrical modes of fixed rotor head turbine.